Original Article

A Practical Method for Slice Spacing Measurement Using the American Association of Physicists in Medicine Computed Tomography Performance Phantom

Choirul Anam, Ariij Naufal, Yanurita Dwihapsari[1], Toshioh Fujibuchi[2], Geoff Dougherty[3]

Department of Physics, Faculty of Sciences and Mathematics, Diponegoro University, Tembalang, Semarang, Central Java, [1]Department of Physics, Faculty of Science and Data Analytics, Sepuluh Nopember Institute of Technology (ITS), Kampus ITS Sukolilo, Surabaya, East Java, Indonesia, [2]Department of Health Sciences, Division of Medical Quantum Sciences, Faculty of Medical Sciences, Kyushu University, Fukuoka, Japan, [3]Department of Applied Physics and Medical Imaging, California State University Channel Islands, Camarillo, CA, USA

Abstract

Background: The slice spacing has a crucial role in the accuracy of computed tomography (CT) images in sagittal and coronal planes. However, there is no practical method for measuring the accuracy of the slice spacing. **Purpose:** This study proposes a novel method to automatically measure the slice spacing using the American Association of Physicists in Medicine (AAPM) CT performance phantom. **Methods:** The AAPM CT performance phantom module 610-04 was used to measure slice spacing. The process of slice spacing measurement involves a pair of axial images of the module containing ramp aluminum objects located at adjacent slice positions. The middle aluminum plate of each image was automatically segmented. Next, the two segmented images were combined to produce one image with two stair objects. The centroid coordinates of two stair objects were automatically determined. Subsequently, the distance between these two centroids was measured to directly indicate the slice spacing. For comparison, the slice spacing was calculated by accessing the slice position attributes from the DICOM header of both images. The proposed method was tested on phantom images with variations in slice spacing and field of view (FOV). **Results:** The results showed that the automatic measurement of slice spacing was quite accurate for all variations of slice spacing and FOV, with average differences of 9.0% and 9.3%, respectively. **Conclusion:** A new automated method for measuring the slice spacing using the AAPM CT phantom was successfully demonstrated and tested for variations of slice spacing and FOV. Slice spacing measurement may be considered an additional parameter to be checked in addition to other established parameters.

Keywords: American Association of Physicists in Medicine phantom, computed tomography, image quality, QA, slice spacing

Received on: 14-11-2023 **Review completed on:** 14-01-2024 **Accepted on:** 19-01-2024 **Published on:** 30-03-2024

Introduction

Computed tomography (CT) is a remarkable medical imaging modality. CT provides excellent and detailed images for diagnostic medicine, image-guided intervention, radiotherapy planning, and assessment of therapeutic outcome.[1-3] As a very complex imaging system, it is very possible that parts of the CT system may not work properly leading to inappropriate image quality for medical purposes.[3] Hence, quality control (QC) procedure should be routinely conducted to guarantee sufficient image quality for a specific task.[4-6] Some of the key image quality parameters commonly used are spatial resolution,[7] low-contrast detectability,[8,9] image noise,[10,11] and uniformity.[12]

Access this article online

Quick Response Code:

Website: www.jmp.org.in

DOI: 10.4103/jmp.jmp_155_23

Apart from image quality, other parameters such as slice thickness[13] and slice spacing (or slice interval) are also very important to establish an accurate diagnosis or other medical needs. In identifying the accuracy of volumetric properties of CT images, for example, the slice thickness accuracy plays an important role.[14,15] Many studies have been performed to evaluate the impact of slice thickness on the accuracy of the

Address for correspondence: Dr. Choirul Anam, Department of Physics, Faculty of Sciences and Mathematics, Diponegoro University, Jl. Prof. Soedarto, SH, Tembalang, Semarang 50275, Central Java, Indonesia.
E-mail: anam@fisika.fsm.undip.ac.id

How to cite this article: Anam C, Naufal A, Dwihapsari Y, Fujibuchi T, Dougherty G. A practical method for slice spacing measurement using the American Association of Physicists in Medicine computed tomography performance phantom. J Med Phys 2024;49:103-9.

volume of cancers[16] and lung nodules.[17] Besides the slice thickness, the slice spacing determines the volume accuracy of a particular organ or object of interest.[18,19] The slice spacing also has a crucial role in the accuracy of the results of 3D image reconstruction for the purpose of visualizing CT images in sagittal and coronal sections.[20] The two parameters (i.e., slice thickness and slice spacing) are fundamentally different and contribute to the accuracy of the volume of organ or object of interest. This is illustrated in Figure 1. Slice thickness refers to the distance on the *z*-axis, which represents the thickness of a slice in a reconstructed axial image, while the slice spacing refers to the distance between two axial images along the *z*-axis.

The slice spacing information can be directly extracted from the DICOM header (i.e., using tag [0018, 0088]: SpacingBetweenSlices). In addition, each image slice has a specific location attribute that can also be accessed through the DICOM header (i.e., using tag [0020, 1041]: SliceLocation). On the same examination, therefore, slice spacing can be calculated from the difference of two adjacent slice locations.

Unlike slice thickness, which has a standard measurement method in a QC program and a standard accuracy criterion, there is still no practical method for measuring slice spacing. This limitation motivated us to propose a method to measure the slice spacing and to develop an algorithm to automatically measure it using a readily available phantom, namely the American Association of Physicists in Medicine (AAPM) CT performance phantom model 610.

Methods

Phantom images

To determine the slice spacing, the 610-04 module of the AAPM CT performance phantom model 610 (CIRS Inc., USA) was used. This module is usually used for slice thickness evaluation. The module is made from three aluminum plates of size 0.635 mm × 25.4 mm,[21] positioned at an angle of 45°. The medium surrounding the aluminum plates is water. When the module is scanned, it produces an axial image in the form of three stair objects. The schematic diagram and axial image of the module are shown in Figure 2.

A method for measuring slice spacing

The measurement of the slice spacing employs two adjacent images with different slice positions of the 610-04 module of the AAPM CT performance phantom. The slice spacing measurement process is depicted in Figure 3.

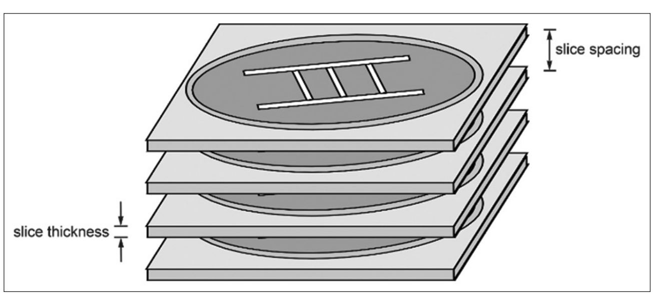

Figure 1: Geometrical relationship of axial plane of phantom images

In the first image (i.e., first slice), the stair object was segmented from the rest objects within the image with a threshold of 200 HU. This segmentation produces a binary image with a foreground of three stair objects. A labeling process was performed to select the middle stair object, and the coordinates of its centroid were automatically determined by Eq. (1).[14]

$$X_{c1} = \frac{1}{|R|}.\sum_{(i,j)\in R} i$$

$$Y_{c1} = \frac{1}{|R|}.\sum_{(i,j)\in R} j \tag{1}$$

where X_{c1} and Y_{c1} are the center coordinates of the foreground stair object in slice #1. R is a region of a binary array that can be interpreted as a two-dimensional object.

In the second image (i.e., second slice) at an adjacent location, the processes of segmentation of the middle stair object and its centroid were also carried out. After that, the two segmented images were combined to produce one image with two stair objects. The slice spacing (d_m) was determined as the distance between the centroid coordinates of two images obtained, namely (X_{c1}, Y_{c1}) and (X_{c2}, Y_{c2}), using Eq. (2).

$$d_m = \sqrt{\left(X_{c1} - X_{c2}\right)^2 + \left(Y_{c1} - Y_{c2}\right)^2} \tag{2}$$

d_m in mm was calculated by multiplying it with the pixel spacing of the image, which was obtained from the DICOM header. Because the stair object is a projection of the aluminum material on the phantom module with a slope of 45°, the d_m directly represents the slice spacing without angle correction.

The proposed method was compared with the slice spacing obtained from the two slice positions extracted from the DICOM header (Eq. [3]).

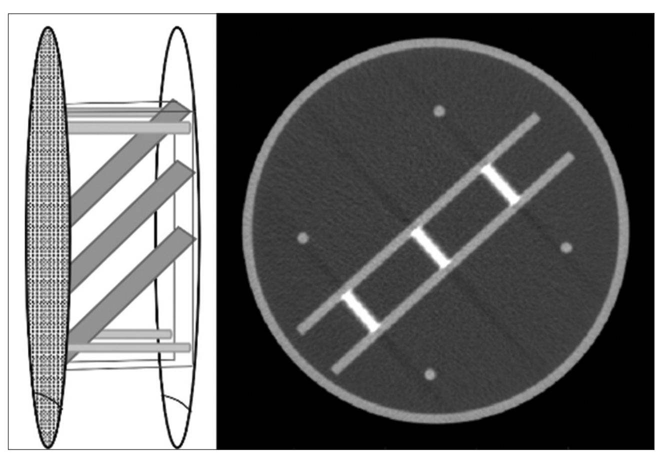

Figure 2: Schematic of 610-04 module of the American Association of Physicists in Medicine computed tomography phantom module 610-04 (left) and its axial image (right)

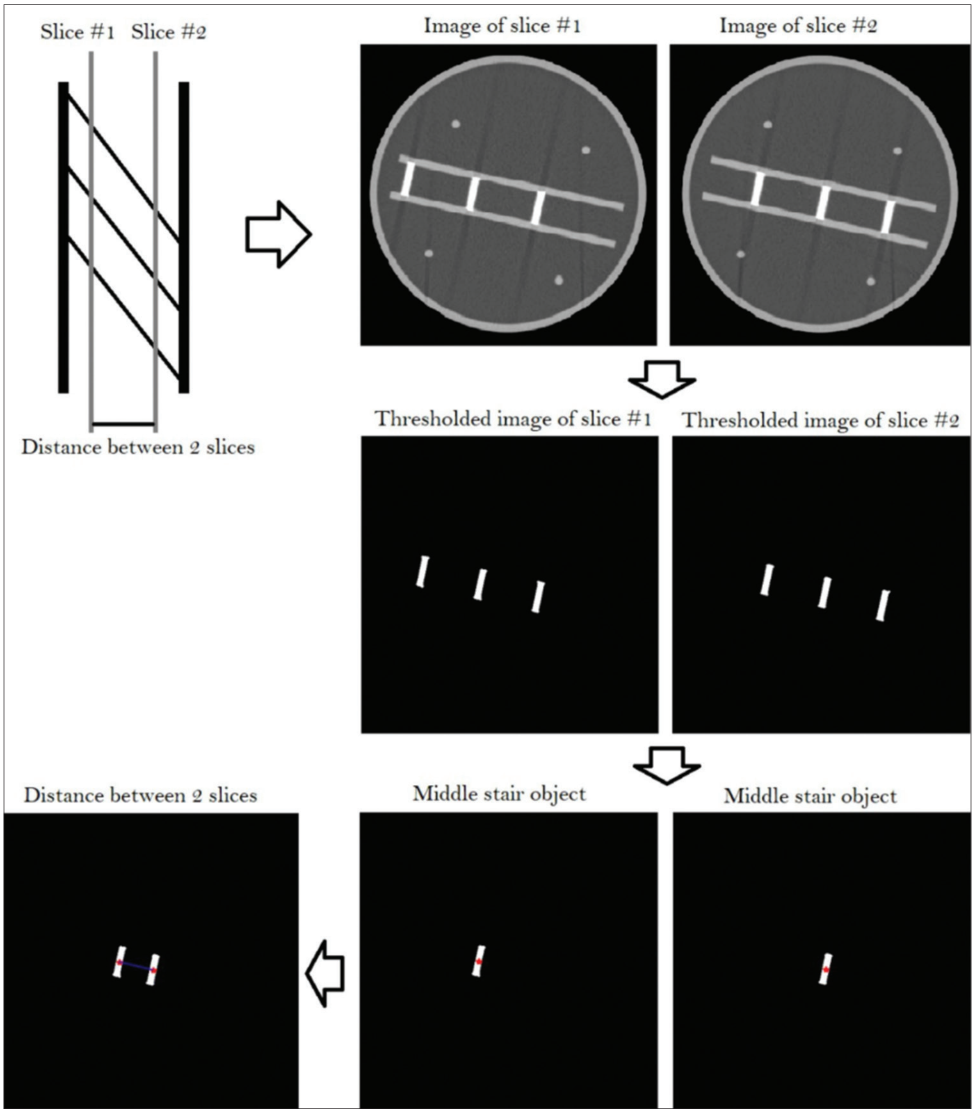

Figure 3: The steps for automated measurement of the distance between two slices

$$d_{set} = |s_1 - s_2| \quad (3)$$

where d_{set} is the set slice spacing in mm, while s_1 and s_2 are the slice positions of the two images which can be obtained from the DICOM header of each image (i.e., using [0020, 1041]: SliceLocation). In addition, the nominal slice spacing can also be directly extracted from the DICOM header (i.e., 0018, 0088: SpacingBetweenSlices).

The difference between d_m and d_{set} shows the deviation of the result of automated measurement and the set distance, using Eq. (4).

$$\Delta d = |d_m - d_{set}| \quad (4)$$

The algorithm was integrated into IndoQCT software written using the Python programming language.[22] A simple graphical user interface was developed for this purpose, as shown in Figure 4. The user is able to freely choose two slices and determine the slice spacing between them.

Data collection and processing

The proposed method was tested on images of the phantom scanned with two scanners, i.e. Philips Ingenuity and a GE Revolution EVO. The evaluation using two different scanners is useful to test the universality of the proposed automatic method for different scanners. There were two variations of parameters tested in our study, i.e., slice spacing and field of view (FOV). The slice spacing was conducted using a GE Revolution EVO scanner (General Electric, US) with slice spacings of 0.625, 1.25, 2.5, 3.75, 5, 7.5, and 10 mm, respectively. The images of the module of the phantom at the respective slice spacing are shown in Figure 5. The nominal slice spacing was automatically calculated using our proposed method and compared with the slice spacing values extracted directly from the DICOM header.

The observation of FOV was performed using the Philips Ingenuity scanner (Philips, The Netherlands) with FOVs of 240, 300, 340, 400, and 440 mm, respectively, and their images are shown in Figure 6. In this study, the measurements of slice spacing were performed on 10 adjacent image pairs, except when the number of slices was not sufficient for module 610-04, such as for several thick slices. After obtaining the measured slice spacing with our proposed method, the nominal slice spacing was accessed from the DICOM header as a comparison. The acquisition parameters for experiment of each variation are tabulated in Table 1.

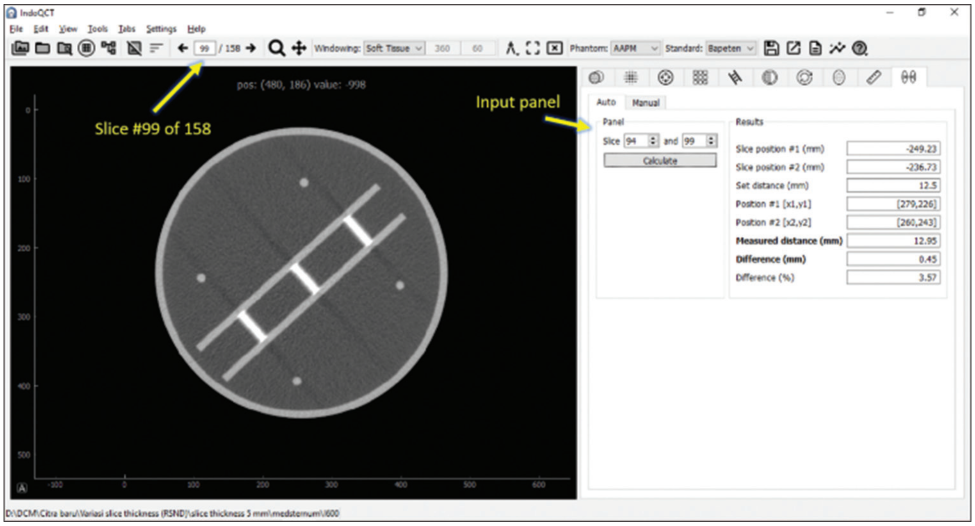

Figure 4: A graphical user interface for the automatic measurement of the slice spacing

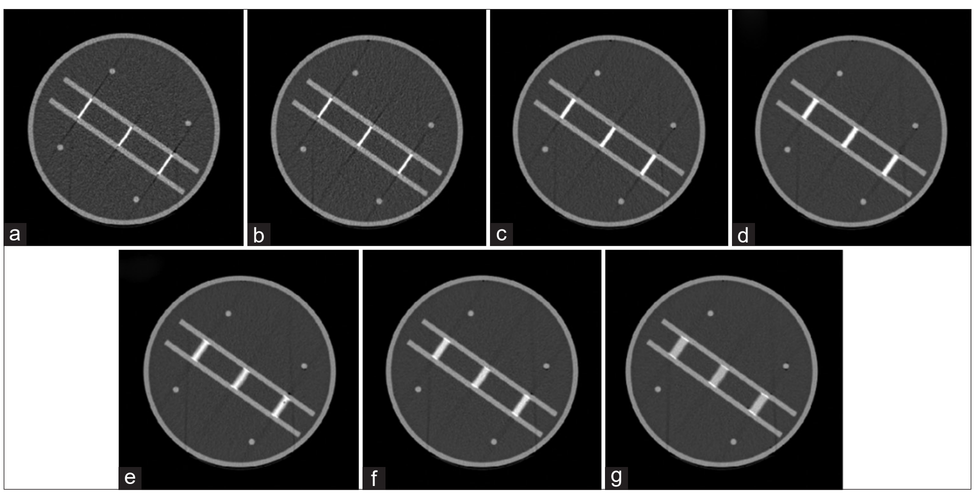

Figure 5: Phantom images (for experiment of slice spacing) at various slice spacings: (a) 0.625 mm, (b) 1.25 mm, (c) 2.5 mm, (d) 3.75 mm, (e) 5 mm, (f) 7.5 mm, and (g) 10 mm

Table 1: Scan parameters for experiments of slice spacing, field of view, and orientation angle variations

Scan parameter	Variation	
	Slice spacing	FOV
Scanner	GE revolution EVO	Philips ingenuity CT
Slice thickness (mm)	0.625, 1.25, 2.5, 3.75, 5, 7.5, and 10	5
Slice spacing between two adjacent images (mm)	0.625, 1.25, 2.5, 3.75, 5, 7.5, and 10	2.5
Tube voltage (kVp)	120	120
Tube current (mA)	100	TCM
Scan mode	Helical	Helical
Pitch	0.96875	1.184
FOV (mm)	272	240, 300, 340, 400, 440
Angle (°)*	125	75

*Angle is phantom's orientation angle. FOV: Field of view, CT: Computed tomography, TCM: Tube current modulation

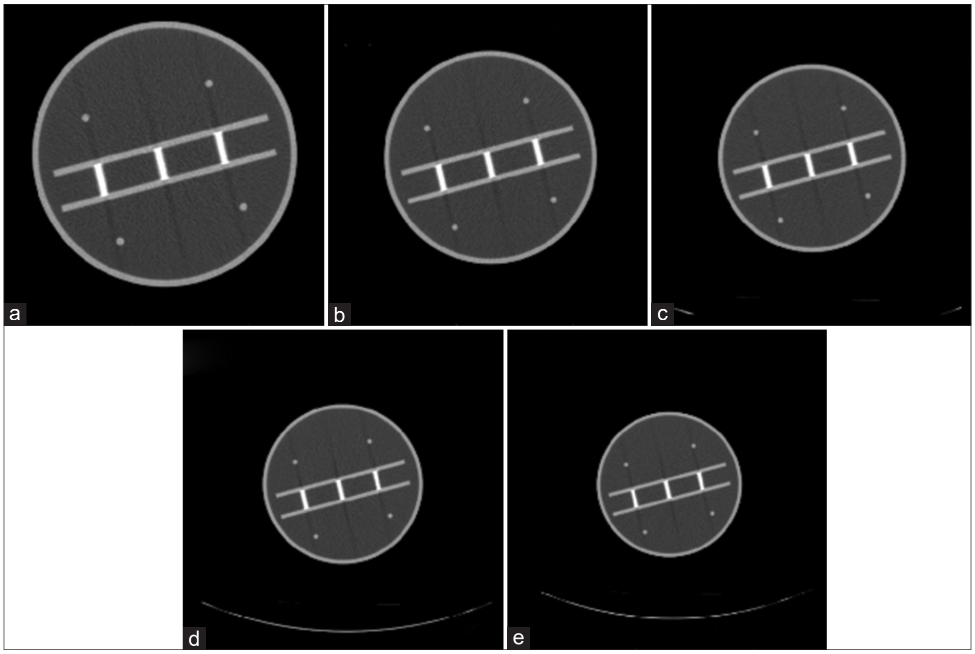

Figure 6: Phantom images at various field of views: (a) 240 mm, (b) 300 mm, (c) 340 mm, (d) 400 mm, and (e) 440 mm

Data analysis

The measured slice spacing was analyzed to find any statistical differences from nominal slice spacing values. The Mann–Whitney *U*-test was used with a significance value of $P = 0.05$. It is found that both data (nominal and measured) are not significantly different for $P > 0.05$.

Results

Variation of slice spacing

At nominal slice spacings of 0.625, 1.25, 2.5, 3.75, 5, 7.5, and 10 mm, slice spacing values extracted directly from the DICOM header and the one calculated from the difference in slice positions (which are also extracted from the DICOM header) show the same value. The percentage error of the automatic measurements of slice spacing at various nominal slice spacings is shown in Figure 7. The measurements were performed on 10 slices for each variation. Figure 7 indicates that the proposed method can accurately measure slice spacing from small to large nominal slice spacing. All the measured slice spacings were fairly close to the nominal values. At thin slice spacing (<2.5 mm), the percent error shows higher results (>10%). In contrast, at thick slice spacing, the percent error is lower (<10%). The average difference for all measurements is 9.0%. From the statistical test, it was found that the measured slice spacing values were not significantly different from the nominal slice spacing values ($P = 0.7$).

Variation of field of view

Figure 8 shows the percentage error of automatic slice spacing measurements for FOV variation with a nominal slice spacing of 2.5 mm. The measurements were performed on 10 slices at each FOV. It shows that, for various FOVs, our method can detect the stair objects from many slices and measure their distances to obtain measured slice spacing. There is no noticeable trend, but the overall error is similar to the variation of slice spacing [Figure 7]. The average difference in all FOVs used is 0.21 mm (9.3%). From the statistical test, it was found that the measured slice spacing values were significantly different from the nominal slice spacing values ($P = 0.001$).

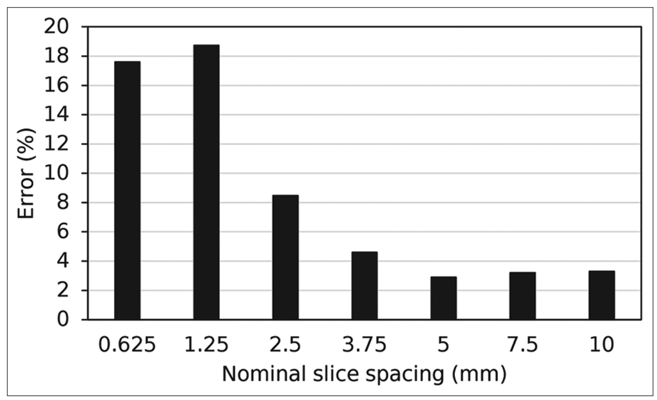

Figure 7: Percentage error of slice spacing measurement at various nominal slice spacings from 0.625 to 10 mm

Discussion

In terms of identifying the volumetric properties of CT images, a very important parameter besides slice thickness is slice spacing.[23] The slice spacing can be used as a benchmark for volumetric measurement accuracy.[19] However, to our knowledge, there is no established methodology for measuring slice spacing. The current study proposes a method to measure the accuracy of the slice spacing and to develop an algorithm

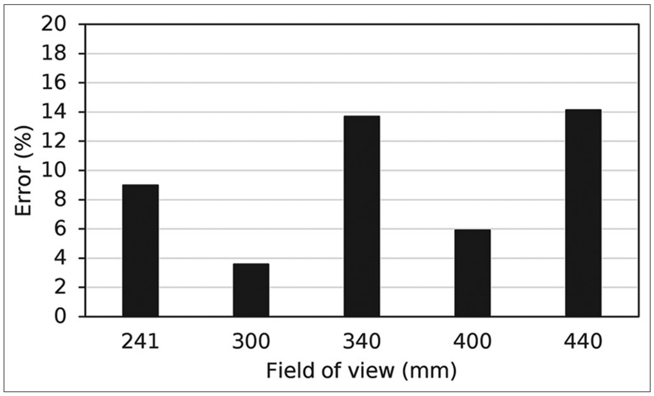

Figure 8: Percentage error of slice spacing measurement for various field of views

to automatically measure it using a readily available phantom, namely the AAPM CT performance phantom.

Slice spacing indicates the distance between two adjacent slices. It can be performed on a pair of images at any location as long as they still show the stair object clearly. In this study, the slice spacing was measured from many image pairs to obtain a measured value automatically. For comparison, slice spacing directly from the DICOM header and from different slice positions extracted from the DICOM header of each image was used. It is noted that the slice spacing information does not always exist in the DICOM header.

The method was tested on the images with variations of slice spacing and FOV. The difference between measured slice spacing and nominal slice spacing is <20%, indicating that the proposed method is quite accurate. For small slice spacing, the measurement results indicate less accurate values since the segmented objects were wider that they should be. For small FOVs, the differences were slightly larger, which may be due to phantom tilting. Based on the FOV data, the FOV in the axial image affects the measured slice spacing. This is because different FOVs result in a different fidelity of reconstructed objects. At small FOVs, the pixel size becomes smaller so that the determination of the centroid of the staircase object becomes less sensitive. In contrast, large FOVs produce images with a large pixel size, leading to a more sensitive centroid determination. The stair object for slice thickness measurement in the AAPM CT performance phantom is designed with a slope of 45° to the *z*-axis.[24] Thus, the slice spacing value does not need to be corrected because of the object angle. However, for other phantoms that have an object tilt angle of less or more than 45°, the distance between the two centroid points needs to be corrected with the angle in order to find the accurate slice spacing.

It is worth noting that the measurement of slice spacing relies on the ramp object. Hence, any improper placement of the phantom leads to inaccuracies of the slice spacing so that the phantom must be positioned accurately on the table. The data were obtained from only two different scanners (Philips Ingenuity CT and GE Revolution EVO). However, the images from the two scanners are limited, so testing the method with more data is needed in any further study. In addition, it is still necessary to compare slice spacing to slice thickness as it is closely related. It is noted that the nominal slice spacing can be reconstructed either equal to the nominal slice thickness or different from it. Regardless, as this initial study shows, the algorithm runs well for images used and shows that the proposed method has the potential to be used as an additional CT scan test.

In our automated method, the distance between slices is only measured on the middle object. It would be better if the user could choose the object freely to anticipate the failure of the segmentation process of the middle stair object. The option of selecting these objects to vary the measurements will be added in future studies. It is also important to fill the phantom carefully with water to avoid the presence of air bubbles that could affect the segmentation results. This would result in inaccurate centroid coordinates, which would lead to inaccuracies in the measurements of the distance between slices. The dataset we used for this paper was derived from helical scans. Further investigation is needed to observe the effect of different scan modes on the robustness of the algorithm and measurement results.

To the best of our knowledge, the current study is the first to develop an algorithm for measuring slice spacing automatically using the 610-04 module of the AAPM CT performance phantom. It is also possible to implement it (with slight modifications) in other CT QA phantoms, such as Philips, Siemens, or other phantoms having a ramp object for measuring slice thickness.

Given the availability of an easy methodology for measuring slice spacing, measurement of this parameter might be considered for inclusion as an integral part of a QC program since the slice spacing parameter is as important as the slice thickness parameter. Regarding the frequency of measurements and the threshold for passing criteria, which are currently not available, it may be possible to use the same frequency and limits for passing criteria as the slice thickness parameter. However, the methodology proposed in this study needs to be evaluated on various CT scanners with various input parameters in future studies. In theory, the proposed method can also be applied to phantom images from other modalities (e.g., magnetic resonance [MR]), as long as the imaging principle is similar (i.e., producing axial images), and the phantoms used contain ramp objects (e.g., using MHR MR imaging phantoms, ramp objects are available for slice profile measurement). Further investigation is needed to evaluate the implementation of the proposed method in other modalities.

Conclusion

A method for measuring slice spacing has been proposed. To increase the effectiveness of measuring this parameter, in-house software for automatic measurement on the AAPM

CT phantom model 610 images was successfully developed. The software accurately measures the slice spacing for various slice spacings and FOVs. The results showed that slice spacing is within 20% of the nominal slice spacing for all variations. It should be noted that the measurement of slice spacing is strongly influenced by the accuracy of the phantom alignment used.

Financial support and sponsorship

This work was funded by the World Class Research University (WCRU), Diponegoro University, 2024.

Conflicts of interest

There are no conflicts of interest.

References

1. Power SP, Moloney F, Twomey M, James K, O'Connor OJ, Maher MM. Computed tomography and patient risk: Facts, perceptions and uncertainties. World J Radiol 2016;8:902-15.
2. Solomon J, Mileto A, Ramirez-Giraldo JC, Samei E. Diagnostic performance of an advanced modeled iterative reconstruction algorithm for low-contrast detectability with a third-generation dual-source multidetector CT scanner: Potential for radiation dose reduction in a multireader study. Radiology 2015;275:735-45.
3. Smith-Bindman R, Lipson J, Marcus R, Kim KP, Mahesh M, Gould R, *et al.* Radiation dose associated with common computed tomography examinations and the associated lifetime attributable risk of cancer. Arch Intern Med 2009;169:2078-86.
4. Nowik P, Bujila R, Poludniowski G, Fransson A. Quality control of CT systems by automated monitoring of key performance indicators: A two-year study. J Appl Clin Med Phys 2015;16:254-65.
5. Anam C, Budi WS, Adi K, Sutanto H, Haryanto F, Ali MH, *et al.* Assessment of patient dose and noise level of clinical CT images: Automated measurements. J Radiol Prot 2019;39:783-93.
6. Roa AM, Andersen HK, Martinsen AC. CT image quality over time: Comparison of image quality for six different CT scanners over a six-year period. J Appl Clin Med Phys 2015;16:4972.
7. Anam C, Fujibuchi T, Budi WS, Haryanto F, Dougherty G. An algorithm for automated modulation transfer function measurement using an edge of a PMMA phantom: Impact of field of view on spatial resolution of CT images. J Appl Clin Med Phys 2018;19:244-52.
8. Baker ME, Dong F, Primak A, Obuchowski NA, Einstein D, Gandhi N, *et al.* Contrast-to-noise ratio and low-contrast object resolution on full- and low-dose MDCT: SAFIRE versus filtered back projection in a low-contrast object phantom and in the liver. AJR Am J Roentgenol 2012;199:8-18.
9. Omigbodun A, Vaishnav JY, Hsieh SS. Rapid measurement of the low contrast detectability of CT scanners. Med Phys 2021;48:1054-63.
10. Christianson O, Winslow J, Frush DP, Samei E. Automated technique to measure noise in clinical CT examinations. AJR Am J Roentgenol 2015;205:W93-9.
11. Anam C, Arif I, Haryanto F, Lestari FP, Widita R, Budi WS, *et al.* An improved method of automated noise measurement system in CT images. J Biomed Phys Eng 2021;11:163-74.
12. Rajendran K, Petersilka M, Henning A, Shanblatt E, Marsh J Jr., Thorne J, *et al.* Full field-of-view, high-resolution, photon-counting detector CT: Technical assessment and initial patient experience. Phys Med Biol 2021;66:205019. [doi: 10.1088/1361-6560/ac155e].
13. Sofiyatun S, Anam C, Zahro UM, Rukmana DA, Dougherty G. An automated measurement of image slice thickness of computed tomography. Atom Indonesia 2021;47:121-8.
14. Greene TC, Rong XJ. Evaluation of techniques for slice sensitivity profile measurement and analysis. J Appl Clin Med Phys 2014;15:4042.
15. Prionas ND, Ray S, Boone JM. Volume assessment accuracy in computed tomography: A phantom study. J Appl Clin Med Phys 2010;11:3037.
16. Luo H, He Y, Jin F, Yang D, Liu X, Ran X, *et al.* Impact of CT slice thickness on volume and dose evaluation during thoracic cancer radiotherapy. Cancer Manag Res 2018;10:3679-86.
17. Narayanan BN, Hardie RC, Kebede TM. Performance analysis of a computer-aided detection system for lung nodules in CT at different slice thicknesses. J Med Imaging (Bellingham) 2018;5:014504.
18. Chadwick JW, Lam EW. The effects of slice thickness and interslice interval on reconstructed cone beam computed tomographic images. Oral Surg Oral Med Oral Pathol Oral Radiol Endod 2010;110:e37-42.
19. Tan Y, Guo P, Mann H, Marley SE, Juanita Scott ML, Schwartz LH, *et al.* Assessing the effect of CT slice interval on unidimensional, bidimensional and volumetric measurements of solid tumours. Cancer Imaging 2012;12:497-505.
20. Wang J, Ye M, Liu Z, Wang C. Precision of cortical bone reconstruction based on 3D CT scans. Comput Med Imaging Graph 2009;33:235-41.
21. Computerized Imaging Reference Systems, Inc. AAPM CT Performance Phantom Model 610: Data Sheet; 2013. Available from: https://www.cirsinc.com/products/diagnostic-ct/aapm-ct-performance-phantom/. [Last accessed on 2011 Feb 11].
22. Anam C, Naufal A, Fujibuchi T, Matsubara K, Dougherty G. Automated development of the contrast-detail curve based on statistical low-contrast detectability in CT images. J Appl Clin Med Phys 2022;23:e13719.
23. Shafiq-Ul-Hassan M, Zhang GG, Latifi K, Ullah G, Hunt DC, Balagurunathan Y, *et al.* Intrinsic dependencies of CT radiomic features on voxel size and number of gray levels. Med Phys 2017;44:1050-62.
24. Lasiyah N, Anam C, Hidayanto E, Dougherty G. Automated procedure for slice thickness verification of computed tomography images: Variations of slice thickness, position from iso-center, and reconstruction filter. J Appl Clin Med Phys 2021;22:313-21.